plant disease

Sclerotinia sclerotiorum infection triggers changes in primary and secondary metabolism in Arabidopsis thaliana

Journal:	*Plant Disease*
Manuscript ID	Draft
Manuscript Type:	Research
Date Submitted by the Author:	n/a
Complete List of Authors:	Chen, Jingyuan; Max-Planck-Institute for Chemical Ecology Ullah, Chhana; Max-Planck-Institute for Chemical Ecology Giddings-Vassao, Daniel; Max-Planck-Institute for Chemical Ecology Reichelt, Michael; Max-Planck-Institute for Chemical Ecology Gershenzon, Jonathan; Max-Planck-Institute for Chemical Ecology Hammerbacher, Almuth; University of Pretoria Forestry and Agricultural Biotechnology Institute, Zoology and Entomology
Keywords:	camalexin, glucosinolates, hydroxycinnamic acid amides, Nδ-acetylornithine, phytohormones, Sclerotinia sclerotiorum

SCHOLARONE™
Manuscripts

Sclerotinia sclerotiorum infection triggers changes in primary and secondary metabolism in *Arabidopsis thaliana*

J. Chen[1], C. Ullah[1], D. G. Vassão[1], M. Reichelt[1], J. Gershenzon[1] and A. Hammerbacher [2*]

[1] Department of Biochemistry, Max Planck Institute for Chemical Ecology, 07745 Jena, Germany

[2] Department of Zoology and Entomology, Forestry and Agricultural Biotechnology Institute, University of Pretoria, Pretoria 0028, South Africa

Corresponding Author: A. Hammerbacher; E-Mail: Almuth.Hammerbacher@fabi.up.ac.za

Running head: *Sclerotinia sclerotiorum* changes plant metabolism

Keywords: camalexin; glucosinolates; hydroxycinnamic acid amides; N^{δ}-acetylornithine; phytohormones; *Sclerotinia sclerotiorum*

Abstract

Sclerotinia sclerotiorum is a devastating plant pathogen that causes substantial losses in various agricultural crops. Although plants have developed some well-known defense mechanisms against invasive fungi, much remains to be learned about plant responses to fungal pathogens. In this study we investigated how plant primary and secondary metabolism in the model plant *Arabidopsis thaliana* are affected by *S. sclerotiorum* infection. Our results showed that the contents of soluble sugars and amino acids changed significantly in *A. thaliana* leaves upon fungal colonization, with a decrease in sucrose and an increase in mannitol, attributed to fungal biosynthesis. Furthermore, the jasmonate signaling pathway was rapidly activated by *S. sclerotiorum* infection, and there was a striking accumulation of antifungal metabolites, such as camalexin, *p*-coumaroyl agmatine, feruloyl agmatine, and N^{δ}-acetylornithine. On the other hand, the characteristic defense compounds of the Brassicaceae, the glucosinolates, were not induced in *A. thaliana* infected by the fungus. Our study provides a better understanding of how *A. thaliana* primary and secondary metabolism are modified during infection by a fungal pathogen like *S. sclerotiorum* that has both hemibiotrophic and necrotrophic stages.

Introduction

Sclerotina sclerotiorum is a destructive pathogen that causes diseases in more than 400 plant species worldwide, including valuable crops such as sunflower, soybean and oilseed rape (Boland & Hall, 1994). This aggressive pathogen has evolved multiple strategies to adapt to diverse environments and host species (Bolton *et al*. 2006; Kabbage *et al*. 2015). On the one hand, formation of sclerotia by hyphal aggregation allows long-term survival of *S. sclerotiorum* under harsh environmental conditions (Abawi & Grogan, 1979). On the other hand, this fungus

secretes numerous enzymes, effectors and toxins to facilitate host colonization (Amselem *et al*. 2011; Kabbage *et al*. 2015). For example, oxalic acid, the most important toxin of *S. sclerotiorum*, enables it to alter reactive oxygen species (ROS) production and programmed cell death in the host plant (Williams *et al*. 2011). Moreover, this fungus has been shown to detoxify plant defense compounds such as flavonols and camalexin, which might assist its expansion in host tissue (Pedras & Hossain, 2006; Chen *et al*., 2019). Further information on the effects of *S. sclerotiorum* on plant physiology and metabolism could suggest new approaches for controlling this challenging agricultural pathogen.

Plants are not defenseless under pathogen attack and have evolved multiple defense mechanisms to protect themselves (Bari & Jones, 2009; Bednarek & Osbourn, 2009; Ahuja *et al*. 2012). Phytohormones are signaling molecules that activate and coordinate plant immune responses (Glazebrook, 2005). In *A. thaliana* jasmonic acid (JA) plays an important role in the defense against infection by necrotrophic pathogens, such as *S. sclerotiorum*. Consequently, a JA- insensitive *coi1* mutant was shown to be more susceptible to *S. sclerotiorum* infection than wild-type plants (Stotz *et al*. 2011a). However, *S. sclerotiorum* has a transient hemi-biotrophic stage during early infection (Williams *et al*. 2011). Therefore, salicylic acid (SA), a hormone generally considered essential for plant defense against biotrophic pathogens, might also be involved in defenses against this pathogen. In support of this hypothesis, the mutation of *npr1* resulting in blocked SA signaling enhanced susceptibility of *A. thaliana* to *S. sclerotiorum* (Guo & Stotz, 2007). Moreover, both SA and abscisic acid (ABA) contents were shown to simultaneously increase upon *S. sclerotiorum* infection in sunflower leaves, although ABA is thought to negatively regulate the JA signaling pathway (Anderson *et al*. 2004). These previous

64 studies suggest that *S. sclerotiorum* infection triggers a complex response of different signaling
65 pathways that requires further clarification.

66 The activation of plant hormone signaling pathways results in the biosynthesis of a
67 variety of secondary metabolites aimed at limiting fungal colonization (Bednarek & Osbourn,
68 2009; Ahuja *et al*. 2012; Ullah *et al*. 2018). Many important secondary metabolites that protect
69 against pathogen infection, such as phenolic acids, flavonoids, anthocyanins and lignin, are
70 synthesized in plants from the amino acid phenylalanine via the phenylpropanoid pathway
71 (Winkel-Shirley, 2001; Dixon *et al*. 2002). The phenylpropanoid pathway also provides a link
72 between the SA signaling pathway, primary metabolism and secondary metabolism (Vogt, 2010;
73 Ullah *et al*. 2018).

74 Other plant secondary metabolites with antifungal activity are products of amino acid
75 biosynthesis, such as N^{δ}-acetylornithine, derived from arginine, glutamate and proline, and
76 camalexin, derived from tryptophan (Adio *et al.*, 2011; Glawischnig *et al*. 2004; Stotz et al,
77 2011b). Glucosinolates (GLs), a group of antifungal and anti-herbivore metabolites specific to
78 the Brassicales order, are biosynthesized from the amino acids methionine and tryptophan in *A.*
79 *thaliana* (Halkier & Gershenzon, 2006). Upon plant tissue damage, GLs are activated by
80 enzymatic hydrolysis to form toxic products known as isothiocyanates, (Halkier & Gershenzon,
81 2006)(Textor & Gershenzon, 2009, Stotz et al, 2011b). GLs are synthesized constitutively in *A.*
82 *thaliana*, but increased amounts are sometimes induced by herbivore invasion (Textor &
83 Gershenzon, 2009).

84 Primary metabolism provides the substrates and energy for plant defense metabolism.
85 However, primary plant metabolites like carbohydrates and amino acids are also important

nutrient sources for pathogens, and are therefore also involved in plant-pathogen interactions (Abood & Losel, 2003, Solomon *et al*, 2003, Jobic *et al*, 2007). A comprehensive study profiling both primary and secondary metabolites during a plant-pathogen interaction could add to our knowledge of how fungi like *S. sclerotiorum* manipulate their host plants and how plants like *A. thaliana* respond.

We used a targeted metabolite profiling approach to investigate the interaction between the model plant *A. thaliana* and *S. sclerotiorum*. Soluble sugars, amino acids, phytohormones, as well as inducible and constitutive specialized defensive metabolites were compared between *S. sclertiorum*-infected and non-infected *A. thaliana* leaves over the course of infection. Our results provide new information about the response of each partner to the other.

Materials and methods

Fungal strain maintenance and plant cultivation

The culture of *S. sclerotiorum* 1980 was maintained on potato dextrose agar (PDA) at 25 °C. A seven-day-old culture was inoculated on PDA and incubated for 2-3 days to obtain vegetative growth. *A. thaliana* wild-type ecotype Columbia (Col-0) was germinated on Murashige and Skoog (MS) medium. One week old seedlings were transferred to potting soil (Klasmann-Deilmann, Geeste, Germany) and grown under short-day conditions (10 h light / 14 h dark cycle at 21 °C, 60% humidity) for 4-5 weeks.

Plant inoculation

Agar plugs (0.5 cm diameter) were punched from the edge of a Petri dish containing actively growing mycelium and placed on 4 fully expanded leaves of 4 - 5 week-old *A. thaliana*

plants. *A. thaliana* inoculated with PDA plugs which did not contain fungus was used as a control (mock inoculation). Inoculation experiments were performed under short-day conditions and each treatment had 4-6 biological replicates. *A. thaliana* plants were harvested at 6 h, 24 h, 48 h and 72 h after inoculation, flash frozen and lyophilized using an Alpha 1-4 LD Plus freeze dryer (Martin Christ GmbH, Osterode, Germany) for 2 days.

Extraction and sample preparation for analysis of primary and secondary metabolites

Lyophilized *A. thaliana* leaves were ground to a fine powder with zirconium oxide beads in a shaking ball mill. Approximately 20 mg plant tissue from each sample was extracted with 1 ml 80% (v v^{-1}) methanol containing 40 ng D4-SA (Santa Cruz Biotechnology, Dallas, TX, USA), 40 ng D6-JA (HPC Standards GmbH, Borsdorf, Germany), 40 ng D6-ABA (Santa Cruz Biotechnology) and 8 ng D6-jasmonoyl isoleucine (D6-JA-Ile, HPLC Standards GmbH) as internal standards for phytohormone quantification, 10 ng trifluoro-methyl-cinnamic acid (Sigma-Aldrich) as an internal standard for phenolic acid quantification, and 50 µM sinalbin (isolated from seeds of *Sinapis alba*) as an internal standard for glucosinolate (GL) quantification. Samples were agitated on a horizontal shaker at room temperature for 10 min and then centrifuged at 18 000 g for 10 min. Approximately 800 µl supernatant was collected into a new microcentrifuge tube. An aliquot of the extract was transferred to a HPLC micro-vial with insert and directly used for phytohormone, phenolic acid, camalexin, coumaroyl agmatine and feruloyl agmatine analysis. A 50 µl aliquot of the extract was mixed with 450 µl water containing 10 µg ml^{-1} [^{13}C, ^{15}N] labeled algal amino acids (Isotec, Miamisburg, OH, USA) as internal standards and used for amino acid quantification. For glucosinolate analysis, a 600 µl portion of the extract was loaded onto a DEAE-Sephadex A-25 (Sigma–Aldrich) column and washed with 0.02 M MES buffer (pH 5.2). Sulfatase solution (arylsulfatase from Sigma-Aldrich) was applied on the

column and incubated at room temperature overnight. Distilled water (500 µl) was used to elute the desulfo-glucosinolates (desulfo-GLs) into 96-deep well plates (Burow *et al*. 2006).

Quantification of primary and secondary metabolites by LC-MS/MS

For soluble sugar analysis, the raw extracts of the samples were diluted 1:10 (v v^{-1}) in water. Glucose, fructose, sucrose and mannitol were measured on an Agilent 1200 series HPLC system (Agilent Technologies) coupled to an API 3200 mass spectrometer (AB Sciex, Darmstadt, Germany). Separation was achieved on an apHera^{TM} NH_2 polymer HPLC column (15 cm × 4.6 mm, 5 µm; Supelco) by water (A) and acetonitrile (B) at a flow rate of 1.0 ml min^{-1} with an elution profile as follows: 0 to 0.5 min, 80% B in A; 0.5 to 13 min, 80% to 55% B; 13 to 14 min, 55% to 80% B; 14 to 18 min, 80% B. Electrospray ionization-MS (ESI) in negative ionization mode was used for detection and quantification. The mass spectrometer parameters were set as follows: ion spray voltage, -4500 V; turbo gas temperature, 600 °C; collision gas, 5 psi; curtain gas, 20 psi; ion source gas 1, 50 psi; ion source gas 2, 60 psi. Precursor and product ions were monitored by scheduled MRM as follows: *m/z* 178.8 →89.0 [collision energy (CE), -10 V; declustering potential (DP), -25 V] at 6.6 min for glucose; *m/z* 178.8 →89 (CE, -7.5 V; DP, -30 V) at 5.6 min for fructose; *m/z* 340.9 →59.0 (CE, -46 V; DP, -45 V) at 8.0 min for sucrose; *m/z* 180.9 →89 at 7 min (CE, -22 V; DP, -35 V) for mannitol. Quantification of these carbohydrates was achieved using external standard curves using commercial standards of D-(-)-fructose, D-(+)-glucose and sucrose (all from Sigma-Aldrich). Mannitol was calculated relative to glucose with an experimentally determined response factor of 0.24.

Amino acids were quantified by LC-MS/MS using a method described previously (Crocoll et al., 2016) with the modification that a QTRAP6500 mass spectrometer (Sciex) was

coupled to the LC system. The analysis involved the coupling of reversed-phase LC by electrospray ionization (ESI) in positive ionization mode to the tandem mass spectrometer operated in MRM mode. For absolute quantification, peak areas of individual amino acids were referenced to the corresponding peaks in the universally labeled ^{13}C, -^{15}N-labeled amino acid internal standard except for tryptophan and asparagine. Tryptophan was quantified using the isotopically labeled phenylalanine using an experimentally determined response factor of 0.42, while asparagine was quantified using the isotopically labeled aspartate as internal standard applying a response factor of 1.0.

Phytohormone analysis was performed on an Agilent 1200 series HPLC system (Agilent Technologies) coupled to a tandem mass spectrometer API 5000 (AB Sciex, Darmstadt, Germany). Separation was achieved on a Zorbax Eclipse XDB-C18 column (50 × 4.6 mm, 1.8 mm; Agilent) with a solvent system of 0.05% formic acid (A) and acetonitrile (B) at a flow rate of 1.1 ml min^{-1}. The elution profile was the following: 0 to 0.5 min, 10% B in A; 0.5 to 4.0 min, 10% to 90% B; 4.0 to 4.02 min, 90% to 100% B, 4.02 to 4.5 min, 100% B and 4.51 to 7.0 min 10% B. ESI-MS in negative ionization mode was used for detection and quantification. The mass spectrometer parameters were set as follows: ion spray voltage, -4500 V; turbo gas temperature, 700 °C; collision gas, 7 psi; curtain gas, 35 psi; ion source gas 1, 60 psi; ion source gas 2, 60 psi. Parent ion to product ion was monitored by multiple reaction monitoring (MRM) as follows: *m/z* 136.9 →93.0 (collision energy [CE], -24 V; declustering potential [DP], -40 V) for SA; *m/z* 299.1 →136.9 (CE, -18 V; DP, -70 V) for SA-glucoside; *m/z* 140.9 →97.0 (CE, -24 V; DP, -40 V) for D_4-SA; *m/z* 290.9 → 165.1 (CE, -24 V; DP, -45 V) for *cis*-oxo-phytodienoic acid (*cis*-OPDA); *m/z* 263.0 → 165.1 (CE, -20 V; DP, -45 V) for *dinor*-OPDA; *m/z* 209.1 →59.0 (CE -24 V; DP -35 V) for JA; *m/z* 225.1 →59.0 (CE, -24 V; DP, -35 V) for OH-JA; *m/z* 305.0 →97.0

(CE, -60 V; DP, -60 V) for sulfo-JA; *m/z* 322.2 →130.1 (CE, -30 V; DP, -50 V) for JA-Ile; *m/z* 338.1 →130.1 (CE, -30 V; DP, -50 V) for OH-JA-Ile; *m/z* 352.1 →130.1 (CE, -30 V; DP, -50 V) for COOH-JA-Ile; *m/z* 263.0 →153.2 (CE, -22 V; DP, -35 V) for ABA; *m/z* 269.0 →159.2 (CE, -22 V; DP, -35 V) for D_6-ABA. Since it was observed that both the D6-labeled JA and D6-labeled JA-Ile standards (HPC Standards GmbH, Cunnersdorf, Germany) contained 40% of the corresponding D5-labeled compounds, the sum of the peak areas of D5- and D6-compounds were used for quantification: sum *m/z* 215.1 →59.0 + *m/z* 214.1 →59.0 (CE -24 V; DP -35 V) for D_6-JA; sum *m/z* 328.2 →130.1+ *m/z* 327.2 →130.1 (CE, -30 V; DP, -50 V) for D6-JA-Ile. Data processing was performed using Analyst 1.5 software and analyte quantity was determined relative to the corresponding internal standard peak area. The concentrations of *cis*-OPDA, *dinor*-OPDA, OH-JA and sulfo-JA were determined relative to the quantity of the internal standard D_6-JA with a theoretical response factor of 1.0. OH-JA-Ile and COOH-JA-Ile were quantified relative to D_6-JA-Ile with a theoretical response factor of 1.0. D4-SA was used for SA-glucoside quantification with a theoretical response factor of 1.0.

Phenolic acids were separated and analyzed with the same LC-MS/MS system described above for phytohormones with a solvent system of 0.1% acetic acid (A) and acetonitrile (B) at a flow rate of 1.1 ml min^{-1}. The elution profile and MS parameters in negative ionization mode were set according to the analysis for phytohormones described above. MRM settings were as follows: *m/z* 147.0 →102.8 (CE, -16 V; DP, -65 V) for *p*-coumaric acid and *m/z* 215.1 →171.1 (CE, -16 V; DP, -65 V) for trifluoro-methyl-cinnamic acid. *p*-Coumaric acid was quantified against the internal standard trifluoro-methyl-cinnamic acid applying an experimentally determined response factor of 4.59.

Analysis of camalexin, coumaroyl agmatine and feruloyl agmatine was achieved on an

198 Agilent 1200 series HPLC system (Agilent Technologies) coupled to a tandem mass
199 spectrometer API 3200 (Applied Biosystems, Darmstadt, Germany) via ESI in positive
200 ionization mode. A Zorbax Eclipse XDB-C18 column was used for separation. 0.05% formic
201 acid and acetonitrile were used as solvent A and B respectively at a flow rate of 1.1 ml min^{-1}
202 with the following profile: 0 to 0.5 min, 5% B in A; 0.5 to 1.0 min, 5% to 100% B ~~in A~~; 1 to 2
203 min, 100% B; 2 to 2.1 min, 100% B to 5% B and 2.1 to 4.5 min 5% B. The MS parameters were
204 optimized as follows: ion spray voltage, 5500 V; turbo gas temperature, 700 °C; collision gas, 4
205 psi; curtain gas, 35 psi; ion source gas 1, 60 psi; ion source gas 2, 60 psi. MRM for the parent ion
206 to product ion was set as follows: *m/z* 201.1 →59.0 (CE, 7.5 V; DP, 51 V) for camalexin; *m/z*
207 277.1 →147.1 (CE, 7.5 V; DP, 30 V) for coumaroyl agmatine; *m/z* 307.1 →177.1 (CE, 7.5 V;
208 DP, 30 V) for feruloyl agmatine. Camalexin concentration was calculated using a camalexin
209 (Sigma-Aldrich) external standard calibration curve. For coumaroyl agmatine and feruloyl
210 agmatine a relative quantification was accomplished and expressed in relative peak area units of
211 the LC-MS/MS signal per mg dry weight.

212 Analysis of GLs was achieved on an Agilent 1100 series HPLC system (Agilent
213 Technologies) with a Nucleodur Sphinx RP C-18 column (250 × 4.6 mm, 5 µm, Macherey-Nagel,
214 Düren, Germany). The mobile phases for desulfo-GLs analysis were water (A) and acetonitrile
215 (B). Compounds were separated using a gradient as follows: 0-1 min, 1.5% B; 1-6 min, 1.5-5%
216 B; 6-8 min, 5-7% B; 8-18 min, 7-21% B; 18-23 min, 21-29% B; 23-24 min, 29-100% B; 24-28
217 min, 1.5% B. GLs were detected using a diode array detector (DAD) as described previously
218 (Burow *et al*. 2006). The peak area of the LC-UV signal at 229 nm was used for quantification of
219 individual GLs against the signal of the internal standard sinalbin using the response factors
220 previously reported (Burow *et al*. 2006).

Identification and quantification of N^{δ}-Acetylornithine

The amino acid extract was further analyzed on an Agilent 1100 series HPLC system (Agilent Technologies, Germany) coupled to an Esquire 6000 ESI-Ion Trap mass spectrometer (Bruker Daltonics, Germany) to identify the new peak that appeared in the MRM chromatogram for determination of arginine by LC-MS/MS of inoculated *A. thaliana* samples. The LC-ESI-IonTrap-MS was operated in alternating ionization mode in the range m/z 60-1000. The MS parameters were set as follows: skimmer voltage, -40 eV; capillary exit voltage, -113.5 eV; capillary voltage, 3500 V; nebulizer pressure, 35 psi; drying gas, 11 L min^{-1}; gas temperature, 330 °C. Elution was accomplished using a EC 250/4.6 Nucleodur Sphinx RP column (25 cm x 4.6 mm, particle size 5 µm, Macherey-Nagel, Germany) with a gradient of 0.2% (v v^{-1}) formic acid (solvent A) and acetonitrile (solvent B) at a flow rate of 1.0 mL min^{-1} at 25 °C as follows: 0 to 5.0 min, 0% B in A; 5.0 to 20.0 min, 0% to 45% B; 20.0 to 20.10 min , 45-100% B; 20.10 to 22.0 min, 100% B; 22.0 to 22.10 min, 100-0% B; 22.10-26.0 min, 0% B. The column was diverted in a ratio 4:1 before reaching the ESI unit. The new compound eluted at 3.5 min, with the MS^2 spectrum in positive mode being different from that of arginine. The structure of the new peak was narrowed down by online database searches (PlantCyc and SciFinder, molecular weight: 174.2). One candidate compound, N^{δ}-acetylornithine, which was induced by jasmonates in *A. thaliana* had been previously described by Adio *et al*. (2011) and Lemarie *et al*. (2015).

An authentic standard of N^{δ}-acetylornithine was kindly provided by Nathalie Marnet and Antoine Gravot (INRA, Rennes-Le Rheu, France). MS^2 spectra and retention time of the new peak and the authentic standard matched (Figure S1). An authentic standard of N^{α}-acetylornithine (Toronto Research Chemicals, Toronto, CA) had a different retention time and a different MS^2 spectrum. For the quantification of the N^{δ}-acetylornithine peak in the LC-MS/MS

analyses for amino acids (MRM: m/z: 175.1/70.1), an experimental response factor relative to isotopically labeled proline was determined as 1.75.

Statistical analysis

Data were analyzed using R version 3.5.1. Data normality and variances were analyzed using the Shapiro-Wilk and Levene's test, respectively. If necessary, data were subjected to square root or log transformations to meet the assumptions of parametric tests. All data were then analyzed by two-way ANOVA with two independent variables "treatment (*S. sclerotiorum* and mock inoculated)" and "time post inoculation".

Results

Sclerotinia sclerotiorum infection increased the accumulation of glucose and mannitol in *A. thaliana* leaves

The availability of soluble sugars in plant tissues and their exchange between the host and the pathogen has an important influence on the development of fungal infection (Abood & Losel, 2003). To determine how levels of simple sugars change in *A. thaliana* leaves over the course of infection by the fungal pathogen *S. sclerotiorum*, we quantified the amounts of fructose, glucose, sucrose and mannitol in both infected and uninfected Arabidopsis leaves. Each sugar exhibited a different pattern. The levels of sucrose were significantly lower in infected than control leaves with both levels declining over the course of infection (Figure 1a). Fructose content was higher in *S. sclerotiorum*-inoculated *A. thaliana* leaves at 24 hours post inoculation (hpi) but was lower at 72 hpi compared to the mock-inoculated plants (Figure 1b). Interestingly, glucose levels were higher in fungal-colonized plant tissues compared to the control leaves throughout the experimental period (Figure 1c). Mannitol, an important sugar alcohol produced by filamentous

fungi was observed to steadily accumulate throughout the infection period reaching concentrations up to 600-fold higher in *S. sclerotiorum*-inoculated leaves compared to the corresponding mock-inoculated leaves at 72 hpi (Figure 1d). These results suggest that metabolism of soluble plant sugars was affected by fungal colonization.

Sclerotinia sclerotiorum* infection changes the levels of soluble amino acids in *A. thaliana

Amino acids play a dominant role in primary metabolism in plants as well as serving as important precursors of secondary metabolites (Sonderby *et al*. 2010; Vogt, 2010). The concentrations of most free proteinogenic amino acids were altered by fungal infection throughout the experimental period (Table 1). The contents of valine, leucine, isoleucine, phenylalanine, tryptophan, tyrosine, lysine, arginine and histidine were significantly higher in *S. sclerotiorum*-inoculated leaves in comparison with mock-treated plants at 48 and 72 hours post inoculation (hpi), which is generally considered to represent the later stages of infection (Table 1). In contrast, the levels of methionine, glycine, and asparagine decreased in fungus-infected leaves compared to uninfected leaves at 72 hpi. Levels of many of the most abundant amino acids, such as alanine, proline, serine, threonine and aspartic acid, did not change due to fungal infection (Table 1).

N^{δ}**-acetylornithine accumulates in *S. sclerotiorum* infected Arabidopsis leaves**

In our targeted analysis of amino acids by LC-MS/MS, we detected an unexpected peak (RT: 0.51 min) in the multiple reaction monitoring (MRM) spectrum for arginine (*m/z* Q1/Q3: 175.1/70.1) that appeared with a very high intensity next to the arginine peak (RT: 0.44 min) in *S. sclerotiorum*-infected samples (Figure 2a). According to the MS^2 fragmentation pattern, retention time and comparison with an authentic standard, the compound was identified as N^{δ}-

acetylornithine (Figure 2b, Figure S1) (Lemarie *et al*. 2015). The possibility of the N^{α}-acetylornithine isomer (acylation on amino group α to carbonyl function) was excluded by analysis of an authentic standard of this compound. N^{δ}-acetylornithine can be synthesized from arginine, glutamic acid and proline (Adio *et al*. 2011). *S. sclerotiorum* infection significantly increased the accumulation of N^{δ}-acetylornithine in *A. thaliana* leaves throughout the experimental period (Figure 2b). The highest accumulation of this compound was found at 48 hpi with approximately 75-fold higher concentrations than in the corresponding mock-inoculated leaves.

S. sclerotiorum infection in _A. thaliana_ leaves induces the jasmonate pathway

Plant hormones such as SA, JA and ABA are involved in plant defense regulation against a range of biotic stresses (Glazebrook, 2005; Bari & Jones, 2009). To determine how these hormone pathways respond to *S. sclerotiorum* infection, we quantified the concentrations of SA, ABA, JA and their relevant metabolites in leaves of *A. thaliana* at different time points after inoculation with *S. sclerotiorum*. SA levels were only slightly affected by *S. sclerotiorum* infection (Figure 3a). SA-glucoside levels also did not change due to fungal infection (Table 2). ABA content increased throughout the experimental period both in control and fungus infected plants (Figure 3b). In contrast, the JA pathway was significantly upregulated by *S. sclerotiorum* infection (Figure 3c-f, Table 2). *cis*-(+)-12-Oxo-phytodienoic acid (*cis*-OPDA) and *dinor*-12-oxo-phytodienoic acid (*dinor*-OPDA) were up to 2-5 fold higher at 24 hpi in infected plants compared to control plants (Figure 3c and d). The levels of JA also increased significantly upon fungal infection, with the highest levels at 24 hpi, which then decreased in inoculated *A. thaliana* leaves but were still substantially higher than in the mock treatment (Figure 3e). A sustained accumulation of JA-Ile was observed in *S. sclerotiorum*-inoculated leaves throughout infection.

311 The concentration of other JA catabolites: 12-hydroxy-JA (OH-JA), 12-hydroxy JA sulfate
312 (sulfo-JA), 12-hydroxy-JA isoleucine conjugate (OH-JA-Ile), and 12-carboxy-JA isoleucine
313 conjugate (COOH-JA-Ile), were also significantly higher in *S. sclerotiorum*-infected leaves
314 compared to control leaves over the course of infection (Table 2).

315 **Arabidopsis alters its secondary metabolite profiles upon *S. sclerotiorum* infection**

316 Several groups of plant secondary metabolites accumulate in tissues infected by fungal
317 pathogens and pay important roles in anti-pathogen defense (Pedras & Adio, 2008; Ahuja *et al*.
318 2012). We analyzed how the profiles of some *A. thaliana* secondary metabolites changed during
319 the interaction with *S. sclerotiorum*. Camalexin accumulated to much higher levels in fungal-
320 infected leaves compared with control leaves from 6 to 72 hpi (Figure 4a). In inoculated *A.*
321 *thaliana* leaves, this phytoalexin increased rapidly after 6 hpi and reached a maximum level (58-
322 fold higher than control) at 24 hpi and then declined.

323 The phenolic acid, *p*-coumaric acid, is a precursor for various phenylpropanoids and
324 flavonoids (Winkel-Shirley, 2001; Vogt, 2010). *S. sclerotiorum* infection led to an increase in *p*-
325 coumaric acid concentration (Figure 4b). However, more substituted phenolic acids such as
326 caffeic and ferulic acid were almost undetectable in both fungus-inoculated and control plants.
327 Interestingly, *p*-coumaroyl agmatine (the conjugate of *p*–coumaric acid and agmatine)
328 accumulated in significantly higher amounts (3.5- to 26-fold higher) in *S. sclerotiorum* infected
329 tissues compared to mock-inoculated tissues (Figure 4c). Similarly, concentrations of the
330 corresponding ferulic acid conjugate, feruloyl agmatine, also increased dramatically (2.3- to 38-
331 fold higher) upon fungal infection (Figure 4d).

Glucosinolates are important defensive metabolites of the Brassicaceae family including Arabidopsis (Halkier & Gershenzon, 2006, Clay *et al*., 2009, Pedras & Hossain, 2011). Both aliphatic and indolic glucosinolates were compared between *S. sclerotiorum*-infected and mock-inoculated *A. thaliana* plants (Figure 5a and b). In general, the contents of glucosinolates decreased upon *S. sclerotiorum* infection, especially at 72 hpi (Figure 5). The reduction of aliphatic glucosinolates in *S. sclerotiorum*-infected leaves was mainly due to the decrease in 3-methylsulfinylpropyl glucosinolate content by approximately 3-fold (Figure 5a). The decrease in the total indolic glucosinolates was due to a reduction in indolyl-3-methyl glucosinolate contents by approximately 2-fold (Figure 5b). The measured concentrations of all individual glucosinolates are shown in Table S1.

Discussion

Knowledge of metabolic changes in a host plant upon pathogen infection can give new insight into plant-pathogen interactions. Therefore we quantified the levels of several classes of primary and secondary metabolites during *S. sclerotiorum* infection of *A. thaliana* including low molecular weight carbohydrates, amino acids, phytohormones, phytoalexins and glucosinolates.

The changes in carbohydrate composition in a plant host during fungal infection may reflect the exchange between the host and the pathogen (Abood & Losel, 2003) or the mobilization of plant resources for a defense response. In our study, the levels of sucrose decreased in infected *A. thaliana* leaves, which might be caused by fungal assimilation and rapid utilization. A previous study showed that *S. sclerotiorum* possesses several major facilitator superfamily (MFS)-type sugar transporters that allow uptake of sugars from the host during infection (Amselem *et al*. 2011). Plant hexoses are utilized by pathogens to support the

biosynthesis of fungal polyols, such as mannitol (Dulermo *et al*. 2009), a compound that increased dramatically during *S. sclerotiorum* infection of *A. thaliana*. Mannitol is found in many filamentous fungi including *S. sclerotiorum* and is important for the protection of fungi from plant reactive oxygen species during infection (Wang & Le Tourneau, 1972).

Phytopathogenic fungi can utilize plant-derived nitrogen sources including nitrate, ammonia, amino acids and proteins (Hoffland *et al*. 1999 and 2000). We observed a significant increase of many of the less abundant amino acids (valine, leucine, isoleucine, phenylalanine, tryptophan, histidine, tyrosine and arginine) in fungus-inoculated *A. thaliana* leaves from 48 to 72 hpi. At this stage of the infection, we speculate that the increase in amino acids is derived from the fungal mycelium rather than from the host plant. The expression of several *S. sclerotiorum* amino acid biosynthesis genes was induced during infection of *Brassica napus* (Li *et al*. 2004). Therefore, the synthesis of these less abundant amino acids in the present study might exploit plant precursors.

In addition to the proteinogenic amino acids, plants also synthesize non-protein amino acids which may have important roles in plant defense against insect herbivores and pathogens (Adio *et al*. 2011; Huang *et al*. 2011). *S. sclerotiorum* infection induced N^{δ}-acetylornithine, which is derived from arginine, glutamic acid and proline in *A. thaliana* leaves (Adio *et al*. 2011). This non-protein amino acid has been shown to be induced in *A. thaliana* by methyl JA treatment as well as infection by *Pseudomonas syringae* and the biotrophic clubroot-disease causing agent, *Plasmodiophora brassicae* (Adio *et al*. 2011; Lemarie *et al*. 2015). The anti-herbivore activity of N^{δ}-acetylornithine was hypothesized to stem from the storage of nitrogen in an unusable form (Adio *et al*. 2011). However, of the three precursor amino acids of N^{δ}-acetylornithine, the levels of proline decreased at 72 hpi in our study, but the levels of the other two precursors, glutamic

377 acid and arginine, were not reduced in infected *A. thaliana* leaves. Therefore, N^{δ}-acetylornithine
378 might have a different mode of action against fungal infection.

379 Plant hormones regulate defense responses against various pathogen infections (Bari &
380 Jones, 2009). In this study, we found that the content of JA and its conjugate JA-Ile were
381 significantly higher in *S. sclerotiorum* infected leaves compared to the mock-treated plants from
382 6 hpi suggesting that JA signaling is important to induce a rapid and sustained defense response
383 during infection by the pathogen. Similarly, the JA biosynthetic intermediates, *cis*-OPDA and
384 *dn*-OPDA, were also dramatically induced by *S. sclerotiorum* infection. A previous study also
385 showed elevated JA and JA-Ile levels in *A. thaliana* infected by *S. sclerotiorum* (Guo and Stotz,
386 2007). We have now analyzed a number of known JA catabolites, including OH-JA, OH-JA-Ile,
387 and COOH-JA-Ile, which were all found to be induced upon *S. sclerotiorum* infection suggesting
388 that both jasmonate biosynthesis and degradation are involved in the plant's response to infection
389 by this fungus. Induction of the JA signaling pathway is a typical plant response to necrotrophic
390 pathogens like *S. sclerotiorum* (Glazebrook, 2005). While this pathogen also undergoes a
391 transient hemi-biotrophic stage early in the infection process (Williams *et al.*, 2011), no
392 substantial changes in SA signaling were found over the time course studied.

393 Plant defense signaling activates the synthesis of various secondary metabolites,
394 including antimicrobial phytoalexins (Chen *et al*. 2006). We observed a substantial increase in *p*-
395 coumaroyl agmatine and feruloyl agmatine concentrations in plants upon *S. sclerotiorum*
396 infection. Both compounds belong to the hydroxycinnamic acid amides (HCAAs), a group of
397 important antifungal substances in many plant species that are formed by the coupling of
398 hydroxycinnamic acid and amines (Muroi *et al*. 2009). However, *p*-coumaric acid, the precursor
399 for these two HCAAs in *A. thaliana*, increased only slightly in response to fungal infection

whereas other phenolic acids were below the detection level. An accumulation of *p*-coumaroyl agmatine and feruloyl agmatine in plants infected by *S. sclerotiorum* has not been previously shown, and the roles of these metabolites *in planta* against the fungus require further investigation.

A rapid and dramatic accumulation of camalexin was observed in *S. sclerotiorum*-inoculated *A. thaliana* leaves, reflecting a rapid chemical defense response upon pathogen infection. Camalexin can, however, be detoxified by *S. sclerotiorum* through glucosylation (Pedras & Hossain, 2006). Therefore, the decline of camalexin concentration in *S. sclerotiorum*-infected plants from 24 to 72 hpi in our study could have resulted from such a detoxification mechanism.

Glucosinolates (GLs) accumulate in the Brassicaceae as protoxins that are activated by hydrolysis upon plant damage and contribute to defense against various herbivores and pathogens (Clay *et al*. 2009; Textor & Gershenzon, 2009). In our study, neither aliphatic GLs nor indolic GLs were induced by fungal infection in *A. thaliana*, suggesting that the biosynthesis of GLs is not an inducible defense mechanism against *S. sclerotiorum*. However, we found that both aliphatic and indolic GL levels decreased significantly in *S. sclerotiorum*-infected leaves at 72 hpi. This fungus was previously shown not to degrade GLs (Pedras & Hossain, 2011), and the decline appears to result from hydrolysis to isothiocyanates by host plant myrosinases followed by fungal cleavage of the isothiocyanates to their corresponding amines (J. Chen, A. Hammerbacher, D. G. Vassão, unpublished results). Interestingly, the reduction in aliphatic and indolic GL concentrations was mostly due to declines in 3-methylsulfinylpropyl GL and indol-3-ylmethyl GL respectively. It was shown that indol-3-ylmethyl GL was reduced in *A. thaliana*

inoculated with the non-adapted pathogens *Blumeria graminis* and *Erysiphe pisi* due to the hydrolysis of indolic GLs (Clay *et al*. 2009).

Taken together, our targeted metabolite profiling approach revealed that major metabolic changes occur in *A. thaliana* during its interaction with *S. sclerotiorum*, from hormone levels to secondary metabolite biosynthesis. Among primary metabolites, fungal colonization dramatically affected sugars and amino acids. Furthermore, we showed a positive correlation between hormone signaling, primarily dominated by the JA signaling pathway, and the biosynthesis of various secondary metabolites, including N^{δ}-acetylornithine, *p*-coumaroyl agmatine, feruloyl agmatine and camalexin. These changes after fungal infection can be investigated further to determine if they represent defense responses by the plant, offensive responses by the fungus, or unavoidable consequences of the infection process.

Acknowledgements

This work was financially supported by the Max Planck Society and China Scholarship Council (CSC, 201406170041). We thank the MPI-CE greenhouse team for maintaining and growing *A. thaliana*. The authentic standard of N^{δ}-acetylornithine was kindly provided by Nathalie Marnet and Antoine Gravot (INRA, Rennes-Le Rheu, France).

References

Abood JK, Losel DM, 2003. Changes in carbohydrate composition of cucumber leaves during the development of powdery mildew infection. *Plant Pathology* **52**, 256-65.

Adie BaT, Perez-Perez J, Perez-Perez MM *et al.*, 2007. ABA is an essential signal for plant resistance to pathogens affecting JA biosynthesis and the activation of defenses in *Arabidopsis*. *The Plant Cell* **19**, 1665-81.

Adio AM, Casteel CL, De Vos M *et al.*, 2011. Biosynthesis and defensive function of N^{δ}-acetylornithine, a jasmonate-induced Arabidopsis metabolite. *The Plant Cell* **23**, 3303-18.

446 Ahuja I, Kissen R, Bones AM, 2012. Phytoalexins in defense against pathogens. *Trends in Plant*
447 *Science* **17**, 73-90.

448 Amselem J, Cuomo CA, Van Kan JA *et al.*, 2011. Genomic analysis of the necrotrophic fungal
449 pathogens *Sclerotinia sclerotiorum* and *Botrytis cinerea*. *PLOS Genetics* **7**, e1002230.

450 Anderson JP, Badruzsaufari E, Schenk PM *et al.*, 2004. Antagonistic interaction between
451 abscisic acid and jasmonate-ethylene signaling pathways modulates defense gene
452 expression and disease resistance in *Arabidopsis*. *The Plant Cell* **16**, 3460-79.

453 Bari R, Jones JD, 2009. Role of plant hormones in plant defence responses. *Plant Molecular*
454 *Biology* **69**, 473-88.

455 Bednarek P, Osbourn A, 2009. Plant-microbe interactions: chemical diversity in plant defense.
456 *Science* **324**, 746-8.

457 Boland GJ, Hall R, 1994. Index of plant hosts of *Sclerotinia sclerotiorum*. *Canadian Journal of*
458 *Plant Pathology-Revue Canadienne De Phytopathologie* **16**, 93-108.

459 Bolton MD, Thomma BP, Nelson BD, 2006. *Sclerotinia sclerotiorum* (Lib.) de Bary: biology
460 and molecular traits of a cosmopolitan pathogen. *Molecular Plant Pathology* **7**, 1-16.

461 Burow M, Muller R, Gershenzon J, Wittstock U, 2006. Altered glucosinolate hydrolysis in
462 genetically engineered *Arabidopsis thaliana* and its influence on the larval development
463 of *Spodoptera littoralis*. *Journal of Chemical Ecology* **32**, 2333-49.

464 Chen H, Jones AD, Howe GA, 2006. Constitutive activation of the jasmonate signaling pathway
465 enhances the production of secondary metabolites in tomato. *FEBS Lett* **580**, 2540-6.

466 Chen J, Ullah C, Reichelt M, Gershenzon J, Hammerbacher A, 2019. *Sclerotinia sclerotiorum*
467 circumvents flavonoid defenses by catabolizing flavonol glycosides and aglycones. *Plant*
468 *Physiology* **180**, 1975-87.

469 Clay NK, Adio AM, Denoux C, Jander G, Ausubel FM, 2009. Glucosinolate metabolites
470 required for an *Arabidopsis* innate immune response. *Science* **323**, 95-101.

471 Dixon RA, Achnine L, Kota P, Liu CJ, Reddy MSS, Wang LJ, 2002. The phenylpropanoid
472 pathway and plant defence - a genomics perspective. *Molecular Plant Pathology* **3**, 371-
473 90.

474 Dulermo T, Rascle C, Chinnici G, Gout E, Bligny R, Cotton P, 2009. Dynamic carbon transfer
475 during pathogenesis of sunflower by the necrotrophic fungus *Botrytis cinerea*: from plant
476 hexoses to mannitol. *New Phytologist* **183**, 1149-62.

477 Glawischnig E, Hansen BG, Olsen CE, Halkier BA, 2004. Camalexin is synthesized from indole-
478 3-acetaidoxime, a key branching point between primary and secondary metabolism in
479 *Arabidopsis*. *Proceedings of the National Academy of Sciences* **101**, 8245-50.

480 Glazebrook J, 2005. Contrasting mechanisms of defense against biotrophic and necrotrophic
481 pathogens. *Annual Review of Phytopathology* **43**, 205-27.

482 Guo X, Stotz HU, 2007. Defense against *Sclerotinia sclerotiorum* in *Arabidopsis* is dependent on
483 jasmonic acid, salicylic acid, and ethylene signaling. *Molecular Plant-Microbe*
484 *Interaction* **20**, 1384-95.

485 Halkier BA, Gershenzon J, 2006. Biology and biochemistry of glucosinolates. *Annual Review of*
486 *Plant Biology* **57**, 303-33.

487 Hoffland E, Jeger MJ, Van Beusichem ML, 2000. Effect of nitrogen supply rate on disease
488 resistance in tomato depends on the pathogen. *Plant and Soil* **218**, 239-47.

489 Hoffland E, Van Beusichem ML, Jeger MJ, 1999. Nitrogen availability and susceptibility of
490 tomato leaves to *Botrytis cinerea*. *Plant and Soil* **210**, 263-72.

491 Huang TF, Jander G, De Vos M, 2011. Non-protein amino acids in plant defense against insect
492 herbivores: Representative cases and opportunities for further functional analysis.
493 *Phytochemistry* **72**, 1531-7.

494 Jobic C, Boisson AM, Gout E *et al.*, 2007. Metabolic processes and carbon nutrient exchanges
495 between host and pathogen sustain the disease development during sunflower infection
496 by *Sclerotinia sclerotiorum*. *Planta* **226**, 251-65.

497 Kabbage M, Yarden O, Dickman MB, 2015. Pathogenic attributes of *Sclerotinia sclerotiorum*:
498 switching from a biotrophic to necrotrophic lifestyle. *Plant Science* **233**, 53-60.

499 Lemarie S, Robert-Seilaniantz A, Lariagon C *et al*., 2015. Both the jasmonic acid and the
500 salicylic acid pathways contribute to resistance to the biotrophic clubroot agent
501 *Plasmodiophora brassicae* in *Arabidopsis*. *Plant and Cell Physiology* **56**, 2158-68.

502 Li R, Rimmer R, Buchwaldt L*, et al.*, 2004. Interaction of *Sclerotinia sclerotiorum* with a
503 resistant *Brassica napus* cultivar: expressed sequence tag analysis identifies genes
504 associated with fungal pathogenesis. *Fungal Genetics and Biology* **41**, 735-53.

505 Muroi A, Ishihara A, Tanaka C *et al.*, 2009. Accumulation of hydroxycinnamic acid amides
506 induced by pathogen infection and identification of agmatine coumaroyltransferase in
507 *Arabidopsis thaliana*. *Planta* **230**, 517-27.

508 Pedras MS, Adio AM, 2008. Phytoalexins and phytoanticipins from the wild crucifers
509 *Thellungiella halophila* and *Arabidopsis thaliana*: rapalexin A, wasalexins and camalexin.
510 *Phytochemistry* **69**, 889-93.

511 Pedras MS, Hossain M, 2006. Metabolism of crucifer phytoalexins in *Sclerotinia sclerotiorum*:
512 detoxification of strongly antifungal compounds involves glucosylation. *Organic and*
513 *Biomolecular Chemistry* **4**, 2581-90.

514 Pedras MS, Hossain S, 2011. Interaction of cruciferous phytoanticipins with plant fungal
515 pathogens: indole glucosinolates are not metabolized but the corresponding desulfo-
516 derivatives and nitriles are. *Phytochemistry* **72**, 2308-16.

517 Solomon PS, Tan KC, Oliver RP, 2003. The nutrient supply of pathogenic fungi; a fertile field
518 for study. *Molecular Plant Pathology* **4**, 203-10.

519 Sonderby IE, Geu-Flores F, Halkier BA, 2010. Biosynthesis of glucosinolates--gene discovery
520 and beyond. *Trends in Plant Science* **15**, 283-90.

521 Stotz HU, Jikumaru Y, Shimada Y *et al.*, 2011a. Jasmonate-dependent and COI1-independent
522 defense responses against *Sclerotinia sclerotiorum* in *Arabidopsis thaliana*: auxin is part
523 of COI1-independent defense signaling. *The Plant Cell Physiology* **52**, 1941-56.

524 Stotz HU, Sawada Y, Shimada Y *et al.*, 2011b. Role of camalexin, indole glucosinolates, and
525 side chain modification of glucosinolate-derived isothiocyanates in defense of
526 *Arabidopsis* against *Sclerotinia sclerotiorum*. *The Plant Journal* **67**, 81-93.

527 Textor S, Gershenzon J, 2009. Herbivore induction of the glucosinolate-myrosinase defense
528 system: major trends, biochemical bases and ecological significance. *Phytochemistry*
529 *Reviews* **8**, 149-70.

530 Ullah C, Tsai CJ, Unsicker SB *et al.*, 2018. Salicylic acid activates poplar defense against the
531 biotrophic rust fungus *Melampsora larici-populina* via increased biosynthesis of catechin
532 and proanthocyanidins. *New Phytologist*.

533 Vogt T, 2010. Phenylpropanoid biosynthesis. *Molecular Plant Pathology* **3**, 2-20.

534 Wang SY, Le Tourneau D, 1972. Mannitol biosynthesis in *Sclerotinia sclerotiorum*. *Archives of*
535 *Microbiology* **81**, 91-9.

536 Williams B, Kabbage M, Kim HJ, Britt R, Dickman MB, 2011. Tipping the balance: *Sclerotinia*
537 *sclerotiorum* secreted oxalic acid suppresses host defenses by manipulating the host
538 redox environment. *PLOS Pathogens* **7**, e1002107.

539 Winkel-Shirley B, 2001. Flavonoid biosynthesis. A colorful model for genetics, biochemistry,
540 cell biology, and biotechnology. *Plant Physiology* **126**, 485-93.

541

542 **Acknowledgements**

543 This work was financially supported by the Max Planck Society and China Scholarship Council

544 (CSC, 201406170041). We thank the MPI-CE greenhouse team for maintaining and growing *A.*

545 *thaliana*. The authentic standard of N^{δ}-acetylornithine was kindly provided by Nathalie Marnet
546 and Antoine Gravot (INRA, Rennes-Le Rheu, France).

547 **Supporting Information legends**

548 **Figure S1** Identification of N^{δ}-acetylornithine in *S. sclerotiorum*-inoculated Arabidopsis.

549 **Table S1** Concentration of individual glucosinolates in *S. sclerotiorum* (*S. s*)-inoculated and
550 mock-inoculated (Control) *A. thaliana* leaves.

551 **Figure legends**

552 **Figure 1** Quantification of soluble sugars including sucrose (a), fructose (b), glucose (c) and
553 mannitol (d) in *A. thaliana* rosette leaves that were either inoculated with *S. sclerotiorum* or
554 mock-inoculated with sterile agar. Sugars were quantified using LC-MS/MS. Data represent
555 mean ± standard error (n=4) and were analyzed by two-way ANOVA (factors: tr = treatment, ti =
556 time post inoculation, and tr × ti = interaction effect). Corresponding *p* values are indicated in the
557 graphs. DW, dry weight.

558 **Table 1** Concentrations of free amino acids in *S. sclerotiorum*-inoculated and mock-inoculated
559 (Control) *A. thaliana* leaves. Data represent mean ± standard error (n=6) and were analyzed by
560 two-way ANOVA (factors: tr = treatment, ti = time post inoculation and tr × ti = interaction
561 effect). Corresponding *p* values are indicated in the table. DW, dry weight.

562 **Figure 2** Quantification of N^{δ}-acetylornithine in *A. thaliana* leaves inoculated with *S.*
563 *sclerotiorum*. (a) Identification of N^{δ}-acetylornithine in infected *A. thaliana* leaves at 48 h after
564 inoculation. A new peak (molecular weight: 174.2) appeared in the LC-MS/MS chromatograms
565 with the same multiple reaction monitoring (MRM) fragment as arginine (m/z Q1/Q3:

175.1/70.1), but a different retention time. The new peak was then identified as N^{δ}-acetylornithine using an authentic standard that showed the same retention time and MS^2 fragmentation pattern as the compound in our extracts; (b) N^{δ}-acetylornithine accumulated in *A. thaliana* leaves infected by *S. sclerotiorum*. Data represent mean ± standard error (n=6) and were analyzed by two-way ANOVA (factors: tr = treatment, ti = time post inoculation and tr × ti = interaction effect). Corresponding p values are indicated in the graph. DW, dry weight.

Figure 3 Phytohormones in *A. thaliana* inoculated with *S. sclerotiorum* and mock-inoculated plants. Hormones and metabolites, including SA (a), ABA (b), *cis*-OPDA (c), *dn*-OPDA (d), JA (e) and JA-Ile (f) in fungus-inoculated and control leaves were analyzed using LC-MS/MS. Data represent mean ± standard error (n=4-6) and were analyzed by two-way ANOVA (factors: tr = treatment, ti = time post inoculation and tr × ti = interaction effect). Corresponding *p* values are indicated in the graphs. SA, salicylic acid; ABA, abscisic acid; *cis*-OPDA, *cis*-(+)-12-oxo-phytodienoic acid; *dn*-OPDA, *dinor*-12-oxo-phytodienoic acid; JA, jasmonic acid; JA-Ile, JA-isoleucine; DW, dry weight.

Table 2 Concentrations of other hormone metabolites in fungus inoculated- and mock-inoculated (Control) *A. thaliana* leaves. Data represent mean ± standard error (n=4-6) and were analyzed by two-way ANOVA (factors: tr = treatment, ti = time post inoculation and tr × ti = interaction effect). Corresponding *p* values are indicated in the table.

Figure 4 Accumulation of selected secondary metabolites including camalexin (a), *p*-coumaric acid (b), *p*-coumaroylagmatine (c) and feruloylagmatine (d) upon *S. sclerotiorum* infection in *A. thaliana* leaves. These compounds were quantified using LC-MS/MS. Data represent mean ± standard error (n=6) and were analyzed by two-way ANOVA (factors: tr = treatment, ti = time

588 post inoculation and tr × ti = interaction effect). Corresponding p values are indicated in the
589 graphs. DW, dry weight.

590 **Figure 5** Quantification of glucosinolates in *A. thaliana* Col-0 leaves inoculated with *S.*
591 *sclerotiorum*. (a) Aliphatic glucosinolates (GLs); (b) Indolic GLs; (c) Sketch of glucosinolate
592 biosynthesis in *A. thaliana*: aliphatic GLs are derived from methionine via side-chain elongation
593 and extended up to six methylene units, leading to the variety of aliphatic GLs in *A. thaliana*
594 Col-0 (Sonderby et al. 2010), while the indolic GLs I3M are derived from tryptophan and can be
595 further modified to 1MOI3G and 4MOI3G by P450 monooxygenases *CYP81Fs* and *O*-
596 methyltransferases (Pfalz et al. 2011). Data represent mean ± standard error (n=6) and were
597 analyzed by two-way ANOVA (factors: tr = treatment, ti = time post inoculation and tr × ti =
598 interaction effect). Corresponding *p* values are indicated in the graphs. 3MSOP, 3-
599 methylsulfinylpropyl glucosinolate (GL); 4MTB, 4-methylthiobutyl GL; 4MSOB, 4-
600 methylsulfinylbutyl GL; 5MSOP, 5-methylsulfinylpentyl GL; 7MSOH, 7-methylsulfinylheptyl
601 GL; 8-methylsulfinyloctyl GL; I3M, indol-3-ylmethyl GL; 1MOI3M, 1-methoxy-indol-3-
602 ylmethyl GL; 4MOI3M, 4-methoxy-indol-3-ylmethyl GL, DW, dry weight.

Table 1 Concentrations of free amino acids in *S. sclerotiorum*-inoculated and mock-inoculated (Control) *A. thaliana* leaves. Data represent mean ± standard error (n=6) and were analyzed by two-way ANOVA (factors: tr = treatment, ti = time post inoculation and tr × ti = interaction effect). Corresponding *p* values are indicated in the table. DW, dry weight.

Amino acid (nmol g^{-1} DW)	Treatment	Time post inoculation				*P* values
		6 h	24 h	48 h	72 h	
Alanine	Control	7.17 ± 0.28	11.05 ± 0.43	11.21 ± 0.60	10.57 ± 0.65	tr: $p = 0.59$ ti: $p < 0.001$ tr × ti: $p = 0.10$
	S. s	8.75 ± 0.74	10.15 ± 0.28	11.169 ± 0.47	10.53 ± 0.50	
Valine	Control	0.89 ± 0.06	0.8 ± 0.05	0.7 ± 0.03	0.76 ± 0.02	tr: $p < 0.001$ ti: $p = 0.002$ tr × ti: $p < 0.001$
	S. s	1.07 ± 0.12	0.93 ± 0.04	1.73 ± 0.18	1.05 ± 0.08	
Leucine	Control	0.67 ± 0.13	0.53 ± 0.06	0.23 ± 0.01	0.24 ± 0.01	tr: $p < 0.001$ ti: $p = 0.002$ tr × ti: $p < 0.001$
	S. s	0.55 ± 0.08	0.41 ± 0.03	0.78 ± 0.07	0.46 ± 0.04	
Isoleucine	Control	0.56 ± 0.05	0.44 ± 0.03	0.31 ± 0.01	0.33 ± 0.02	tr: $p < 0.001$ ti: $p = 0.002$ tr × ti: $p < 0.001$
	S. s	0.62 ± 0.09	0.46 ± 0.03	0.88 ± 0.10	0.5 ± 0.04	
Proline	Control	1.75 ± 0.13	1.71 ± 0.10	1.49 ± 0.10	2.52 ± 0.19	tr: $p = 0.90$ ti: $p = 0.22$ tr × ti: $p < 0.001$
	S. s	2.51 ± 0.53	1.91 ± 0.13	1.88 ± 0.25	1.41 ± 0.09	
Phenylalanine	Control	0.76 ± 0.07	0.57 ± 0.04	0.49 ± 0.03	0.41 ± 0.02	tr: $p < 0.001$ ti: $p < 0.001$ tr × ti: $p < 0.001$
	S.s	0.89 ± 0.09	0.71 ± 0.02	1.42 ± 0.11	0.98 ± 0.08	
Tryptophan	Control	0.1 ± 0.01	0.09 ± 0.01	0.08 ± 0.00	0.07 ± 0.00	tr: $p < 0.001$ ti: $p < 0.001$ tr × ti: $p < 0.001$
	S. s	0.13 ± 0.02	0.1 ± 0.00	0.21 ± 0.02	0.12 ± 0.01	
Methionine	Control	0.31 ± 0.02	0.35 ± 0.01	0.31 ± 0.02	0.38 ± 0.02	tr: $p < 0.001$ ti: $p = 0.014$ tr × ti: $p < 0.001$
	S. s	0.28 ± 0.01	0.22 ± 0.01	0.35 ± 0.02	0.27 ± 0.01	
Glycine	Control	4.75 ± 0.23	5.08 ± 0.22	4.68 ± 0.17	4.8 ± 0.49	tr: $p = 0.015$ ti: $p = 0.004$ tr × ti: $p = 0.11$
	S. s	5.51 ± 0.45	4.22 ± 0.12	3.96 ± 0.22	3.36 ± 0.49	
Serine	Control	14.43 ± 0.69	12.89 ± 0.51	14.09 ± 0.75	14.9 ± 0.85	tr: $p = 0.81$ ti: $p < 0.001$ tr × ti: $p < 0.001$
	S. s	16.79 ± 1.15	12.01 ± 0.58	16.65 ± 1.16	10.88 ± 0.70	

Table 1 (Continue)

Amino acid (nmol g^{-1} DW)	Treatment	Time post inoculation				*P* values
		6 h	24 h	48 h	72 h	
Threonine	Control	8.62 ± 0.31	7.08 ± 0.20	6.64 ± 0.43	7.16 ± 0.27	tr: $p = 0.20$ ti: $p < 0.001$ tr × ti: $p = 0.004$
	S. s	9.98 ± 0.96	6.15 ± 0.27	6.95 ± 0.45	5.43 ± 0.32	
Tyrosine	Control	0.17 ± 0.01	0.12 ± 0.01	0.11 ± 0.01	0.11 ± 0.01	tr: $p < 0.001$ ti: $p < 0.001$ tr × ti: $p < 0.001$
	S. s	0.2 ± 0.01	0.22 ± 0.01	0.49 ± 0.02	0.43 ± 0.02	
Asparagine	Control	4.75 ± 0.23	5.08 ± 0.22	4.68 ± 0.17	4.8 ± 0.49	tr: $p = 0.012$ ti: $p = 0.012$ tr × ti: $p = 0.012$
	S. s	5.51 ± 0.45	4.22 ± 0.12	3.69 ± 0.22	3.36 ± 0.49	
Lysine	Control	0.46 ± 0.08	0.44 ± 0.03	0.32 ± 0.02	0.29 ± 0.01	tr: $p < 0.001$ ti: $p < 0.001$ tr × ti: $p < 0.001$
	S. s	0.45 ± 0.04	0.58 ± 0.05	1.26 ± 0.07	1.16 ± 0.11	
Arginine	Control	0.76 ± 0.12	0.90 ± 0.04	0.73 ± 0.07	0.42 ± 0.04	tr: $p < 0.001$ ti: $p = 0.015$ tr × ti: $p < 0.001$
	S. s	0.81 ± 0.09	0.93 ± 0.10	1.46 ± 0.22	1.12 ± 0.15	
Histidine	Control	2.14 ± 0.09	2.42 ± 0.09	1.96 ± 0.11	2.2 ± 0.05	tr: $p < 0.001$ ti: $p = 0.003$ tr × ti: $p < 0.001$
	S. s	2.61 ± 0.12	2.17 ± 0.15	3.27 ± 0.13	3.5 ± 0.31	
Aspartic acid	Control	4.86 ± 0.16	4.49 ± 0.16	4.47 ± 0.16	4.75 ± 0.19	tr: $p = 0.88$ ti: $p = 0.48$ tr × ti: $p = 0.83$
	S. s	4.75 ± 0.35	4.48 ± 0.19	4.76 ± 0.18	4.78 ± 0.27	
Glutamic acid	Control	35.5 ± 1.43	38.62 ± 1.42	36.05 ± 1.51	40.22 ± 1.81	tr: $p = 0.014$ ti: $p = 0.49$ tr × ti: $p = 0.11$
	S. s	41.79 ± 2.17	37.77 ± 1.01	42.01 ± 1.65	41.37 ± 2.52	

Table 2 Concentrations of hormone catabolites in fungus inoculated- and mock-inoculated (Control) *A. thaliana* leaves. Data represent mean ± standard error (n=4-6) and were analyzed by two-way ANOVA (factors: tr = treatment, ti = time post inoculation and tr × ti = interaction effect). Corresponding *p* values are indicated in the table. DW, dry weight.

Phytohormone metabolites (ng g-1 DW)	**Treatment**	**Time post inoculation**				***P* values**
		6 h	**24 h**	**48 h**	**72 h**	
OH-JA	Control	764.82 ± 35.52	839.94 ± 140.18	720.19 ± 50.66	217.82 ± 26.93	tr: $p < 0.001$ ti: $p < 0.001$ tr × ti: $p < 0.001$
	S. s	1813.27 ± 340.73	13374.26 ± 960.77	34959.16 ± 1327.22	42698.11 ± 1271.89	
OH-JA-Ile	Control	26.56 ± 0.67	24.92 ± 4.06	23.67 ± 1.88	9.43 ± 2.20	tr: $p < 0.001$ ti: $p < 0.001$ tr × ti: $p < 0.001$
	S. s	81.16 ± 4.19	82.60 ± 15.47	225.80 ± 26.97	293.64 ± 31.10	
COOH-JA-Ile	Control	91.52 ± 2.66	70.16 ± 8.63	65.70 ± 5.60	15.89 ± 1.97	tr: $p < 0.001$ ti: $p = 0.01$ tr × ti: $p < 0.001$
	S. s	170.98 ± 20.36	113.77 ± 15.01	109.86 ± 12.60	169.92 ± 28.30	
Sulfo-JA	Control	5470.99 ± 200.14	6003.06 ± 660.65	6047.77 ± 684.56	3200.23 ± 134.18	tr: $p < 0.001$ ti: $p = 0.52$ tr × ti: $p < 0.001$
	S. s	8380.52 ± 963.40	6933.44 ± 1029.80	8839.05 ± 426.11	12829.94 ± 1038.27	
SA-Glucoside	Control	3535.47 ± 222.58	3412.37 ± 170.75	4041.65 ± 214.67	4202.05 ± 65.48	tr: $p = 0.20$ ti: $p = 0.21$ tr × ti: $p = 0.019$
	S. s	3708.95 ± 231.81	4621.43 ± 366.04	4268.19 ± 500.33	3555.01 ± 236.27	

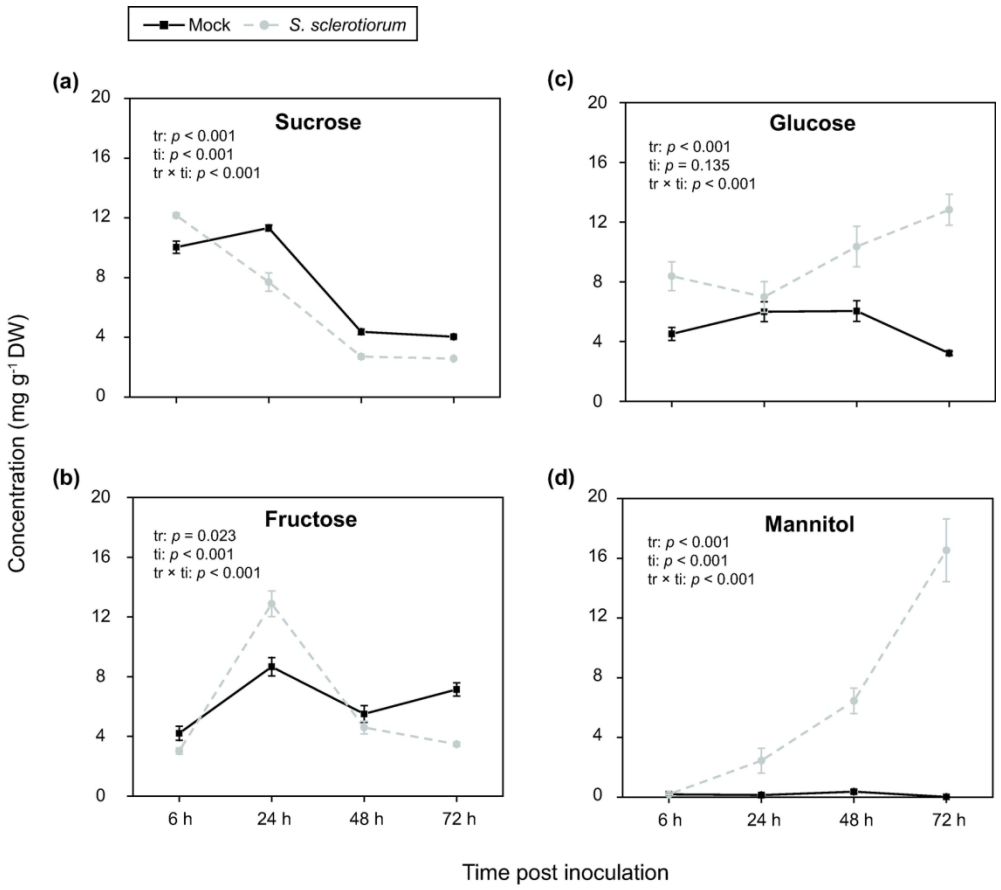

Figure 1 Quantification of soluble sugars including sucrose (a), fructose (b), glucose (c) and mannitol (d) in A. thaliana rosette leaves that were either inoculated with S. sclerotiorum or mock-inoculated with sterile agar. Sugars were quantified using LC-MS/MS. Data represent mean ± standard error (n=4) and were analyzed by two-way ANOVA (factors: tr = treatment, ti = time post inoculation, and tr × ti = interaction effect). Corresponding p values are indicated in the graphs. DW, dry weight.

159x140mm (300 x 300 DPI)

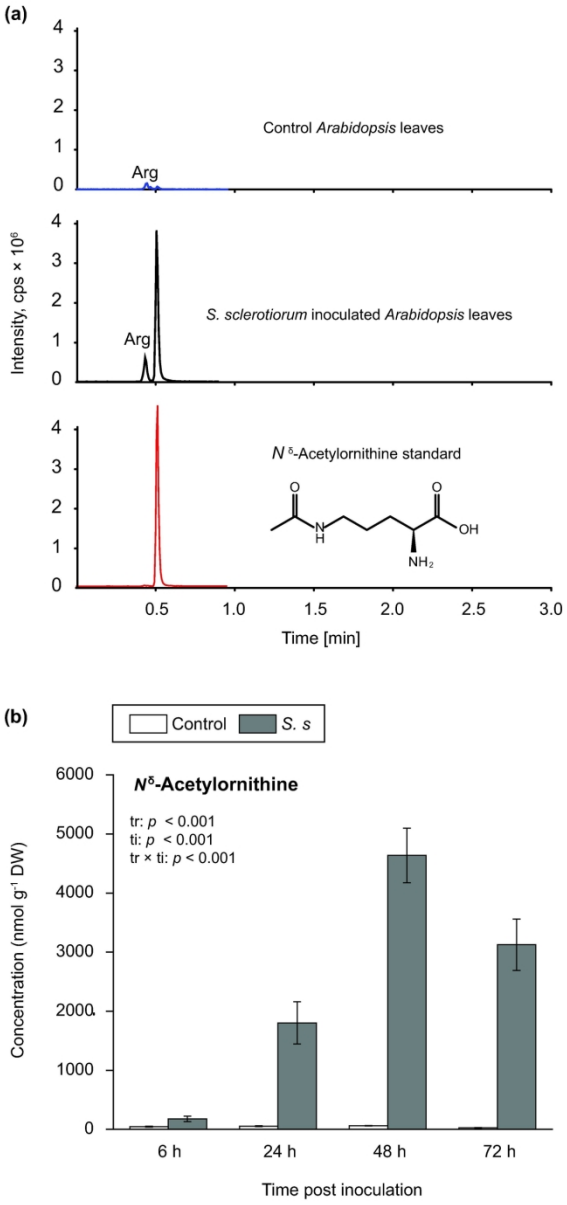

Figure 2 Quantification of Nδ-acetylornithine in A. thaliana leaves inoculated with S. sclerotiorum. (a) Identification of Nδ-acetylornithine in infected A. thaliana leaves at 48 h after inoculation. A new peak (molecular weight: 174.2) appeared in the LC-MS/MS chromatograms with the same multiple reaction monitoring (MRM) fragment as arginine (m/z Q1/Q3: 175.1/70.1), but a different retention time. The new peak was then identified as Nδ-acetylornithine using an authentic standard that showed the same retention time and MS2 fragmentation pattern as the compound in our extracts; (b) Nδ-acetylornithine accumulated in A. thaliana leaves infected by S. sclerotiorum. Data represent mean ± standard error (n=6) and were analyzed by two-way ANOVA (factors: tr = treatment, ti = time post inoculation and tr × ti = interaction effect). Corresponding p values are indicated in the graph. DW, dry weight.

103x222mm (300 x 300 DPI)

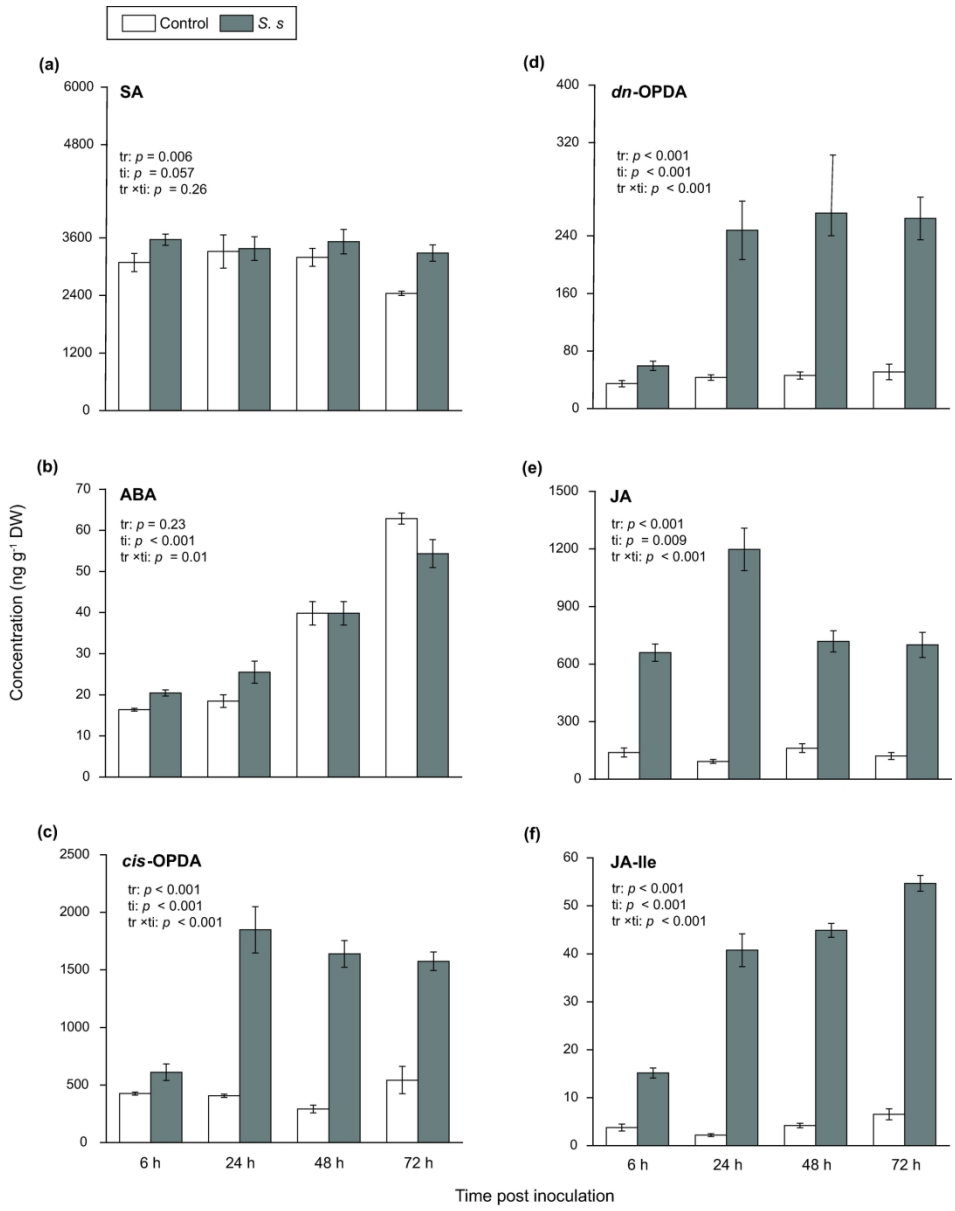

Figure 3 Phytohormones in A. thaliana inoculated with S. sclerotiorum and mock-inoculated plants. Hormones and metabolites, including SA (a), ABA (b), cis-OPDA (c), dn-OPDA (d), JA (e) and JA-Ile (f) in fungus-inoculated and control leaves were analyzed using LC-MS/MS. Data represent mean ± standard error (n=4-6) and were analyzed by two-way ANOVA (factors: tr = treatment, ti = time post inoculation and tr × ti = interaction effect). Corresponding p values are indicated in the graphs. SA, salicylic acid; ABA, abscisic acid; cis-OPDA, cis-(+)-12-oxo-phytodienoic acid; dn-OPDA, dinor-12-oxo-phytodienoic acid; JA, jasmonic acid; JA-Ile, JA- isoleucine; DW, dry weight.

197x249mm (300 x 300 DPI)

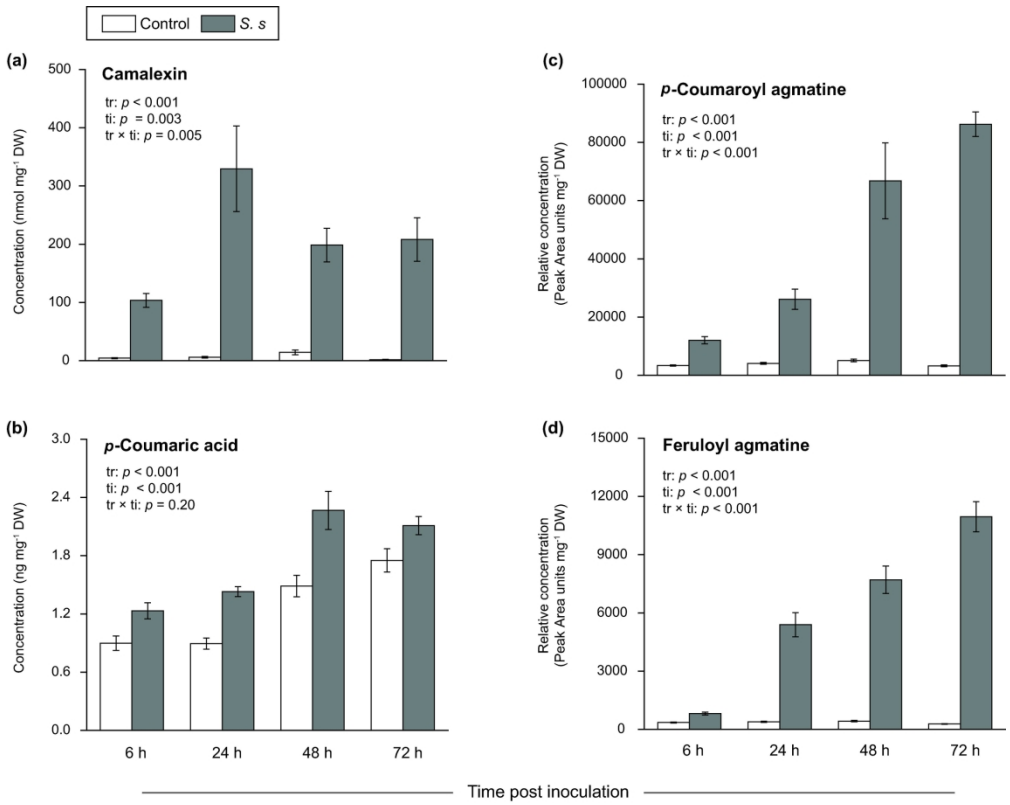

Figure 4 Accumulation of selected secondary metabolites including camalexin (a), p-coumaric acid (b), p-coumaroylagmatine (c) and feruloylagmatine (d) upon S. sclerotiorum infection in A. thaliana leaves. These compounds were quantified using LC-MS/MS. Data represent mean ± standard error (n=6) and were analyzed by two-way ANOVA (factors: tr = treatment, ti = time post inoculation and tr × ti = interaction effect). Corresponding p values are indicated in the graphs. DW, dry weight.

204x163mm (300 x 300 DPI)

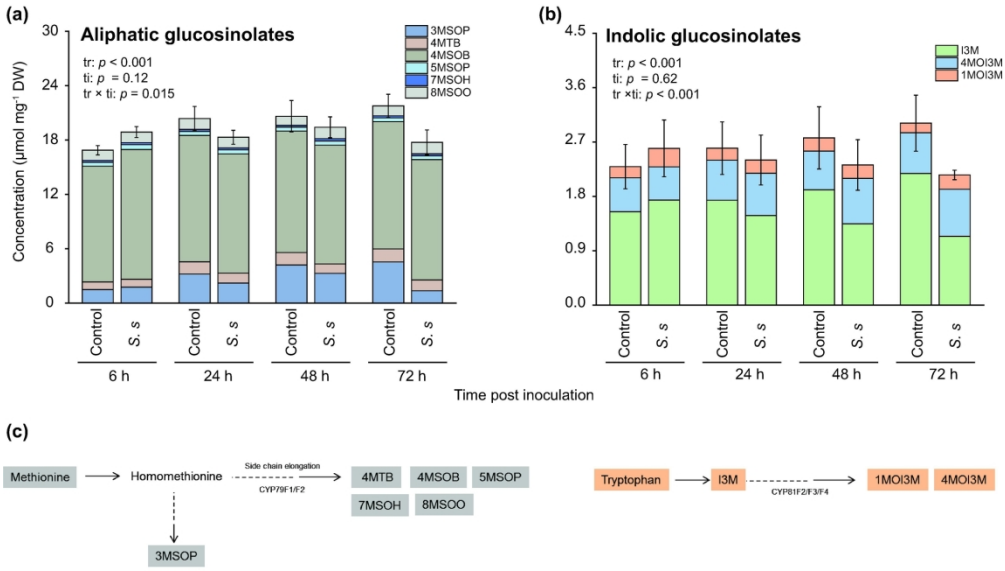

Figure 5 Quantification of glucosinolates in A. thaliana Col-0 leaves inoculated with S. sclerotiorum. (a) Aliphatic glucosinolates (GLs); (b) Indolic GLs; (c) Sketch of glucosinolate biosynthesis in A. thaliana: aliphatic GLs are derived from methionine via side-chain elongation and extended up to six methylene units, leading to the variety of aliphatic GLs in A. thaliana Col-0 (Sonderby et al. 2010), while the indolic GLs I3M are derived from tryptophan and can be further modified to 1MOI3G and 4MOI3G by P450 monooxygenases CYP81Fs and O-methyltransferases (Pfalz et al. 2011). Data represent mean ± standard error (n=6) and were analyzed by two-way ANOVA (factors: tr = treatment, ti = time post inoculation and tr × ti = interaction effect). Corresponding p values are indicated in the graphs. 3MSOP, 3-methylsulfinylpropyl glucosinolate (GL); 4MTB, 4-methylthiobutyl GL; 4MSOB, 4-methylsulfinylbutyl GL; 5MSOP, 5-methylsulfinylpentyl GL; 7MSOH, 7-methylsulfinylheptyl GL; 8-methylsulfinyloctyl GL; I3M, indol-3-ylmethyl GL; 1MOI3M, 1-methoxy-indol-3-ylmethyl GL; 4MOI3M, 4-methoxy-indol-3-ylmethyl GL, DW, dry weight.

189x109mm (300 x 300 DPI)

Supporting Information

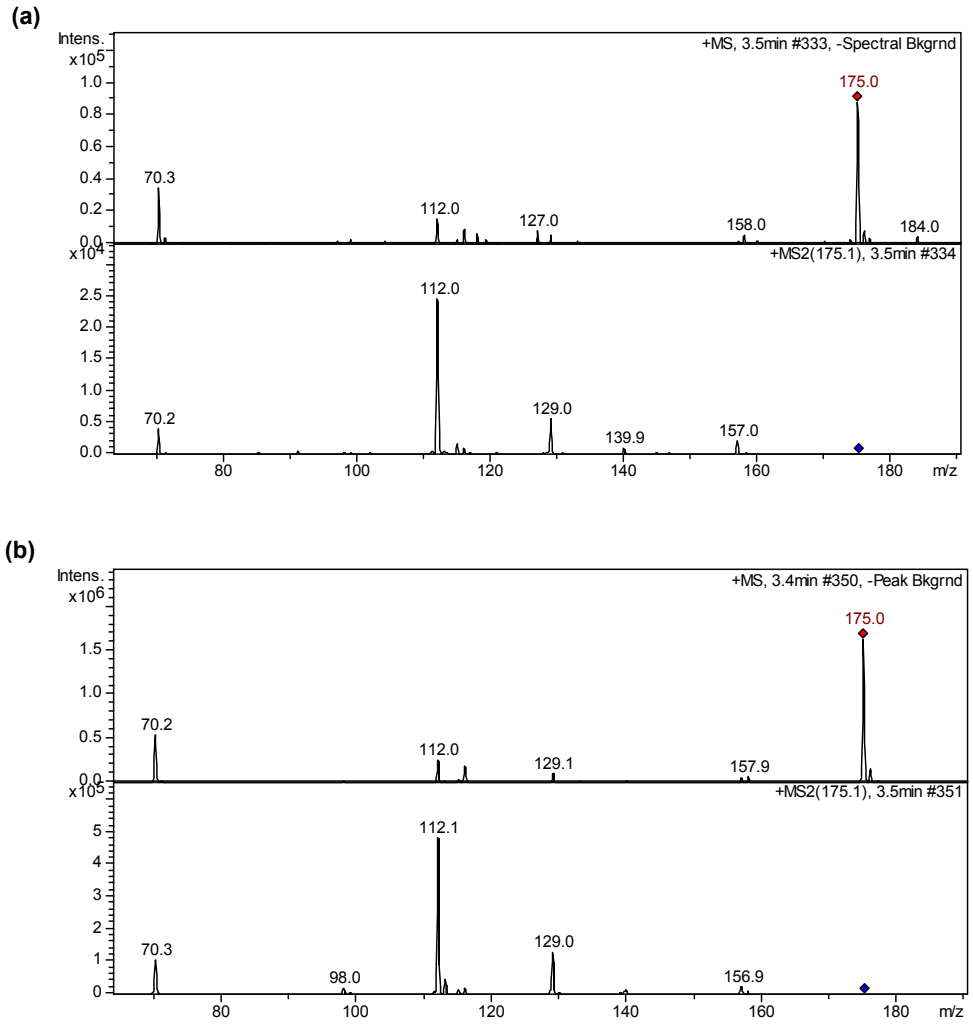

Figure S1. Identification of N^{δ}-acetylornithine in *S. sclerotiorum*-inoculated Arabidopsis. Full scan MS spectrum and MS^2 spectrum (fragmentation spectrum of *m*/*z* 175) in positive ionization mode of N^{δ}-acetylornithine from (a) *S. sclerotiorum* inoculated *A. thaliana* leaf sample and (b) authentic standard

Table S1. Concentration of individual glucosinolates in *S. sclerotiorum* (*S. s*)-inoculated and mock-inoculated (Control) *A. thaliana* leaves. 3MSOP, 3-methylsulfinylpropyl glucosinolate (GL); 4MTB, 4-methylthiobutyl GL; 4MSOB, 4-methylsulfinylbutyl GL; 5MSOP, 5-methylsulfinylpentyl GL; 7MSOH, 7-methylsulfinylheptyl GL; 8-methylsulfinyloctyl GL; I3M, indol-3-ylmethyl GL; 1MOI3M, 1-methoxy-indol-3-ylmethyl GL; 4MOI3M, 4-methoxy-indol-3-ylmethyl GL, DW, dry weight.

Glucosinolates (µmol g^{-1} DW)	**Treatment**	**Time post inoculation**			
		6 h	**24 h**	**48 h**	**72 h**
3MSOP	Control	1.49 ± 0.03	3.21 ± 0.55	4.21 ± 0.62	4.55 ± 0.61
	S.s	1.77 ± 0.06	2.21 ± 0.16	3.28 ± 0.29	1.35 ± 0.10
4MTB	Control	0.84 ± 0.04	1.35 ± 0.04	1.37 ± 0.07	1.43 ± 0.11
	S.s	0.86 ± 0.07	1.11 ± 0.04	1.04 ± 0.13	1.21 ± 0.05
4MSOB	Control	12.79 ± 0.37	13.95 ± 0.67	13.40 ± 0.93	14.06 ± 0.49
	S.s	14.33 ± 0.44	13.16 ± 0.49	13.12 ± 0.60	13.29 ± 1.11
5MSOP	Control	0.44 ± 0.01	0.44 ± 0.02	0.44 ± 0.03	0.42 ± 0.02
	S.s	0.53 ± 0.02	0.44 ± 0.02	0.46 ± 0.03	0.41 ± 0.03
7MSOH	Control	0.20 ± 0.01	0.22 ± 0.01	0.20 ± 0.01	0.22 ± 0.01
	S.s	0.22 ± 0.01	0.22 ± 0.01	0.25 ± 0.01	0.23 ± 0.01
8MSOO	Control	1.13 ± 0.06	1.20 ± 0.06	1.00 ± 0.07	1.09 ± 0.06
	S.s	1.18 ± 0.01	1.18 ± 0.06	1.26 ± 0.08	1.26 ± 0.07
I3M	Control	1.55 ± 0.02	1.74 ± 0.06	1.91 ± 0.12	2.18 ± 0.05
	S.s	1.74 ± 0.12	1.48 ± 0.06	1.35 ± 0.08	1.14 ± 0.05
4MOI3M	Control	0.56 ± 0.02	0.66 ± 0.03	0.64 ± 0.03	0.67 ± 0.02
	S.s	0.55 ± 0.02	0.70 ± 0.03	0.75 ± 0.02	0.78 ± 0.02
1MOI3M	Control	0.18 ± 0.02	0.20 ± 0.01	0.22 ± 0.02	0.16 ± 0.01
	S.s	0.31 ± 0.08	0.22 ± 0.04	0.22 ± 0.02	0.24 ± 0.01